

Supporting Information

pH-Regulated Camouflage Strategy for Access Control in Molecular Systems

DeChun Tian,^{†a} Peijun Shi,^{†b} Xiaokang Zhang,^b Lijun Sun,^b Bin Wang^a and Qiang Zhang^{*b}

^a Key Laboratory of Advanced Design and Intelligent Computing, Ministry of Education, School of Software Engineering, Dalian University, Dalian 116622, China

^b Key Laboratory of Social Computing and Cognitive Intelligence, Ministry of Education, School of Computer Science and Technology, Dalian University of Technology, Dalian 116024, China

*Corresponding author.

E-mail address: zhangq@dlu.edu.cn (Q. Zhang).

[†] These authors contributed equally.

Table of Contents

Supporting Information	1
Table of Contents	1
Materials and Methods.....	1
Supplementary Figures	3
1. Design and structural optimization of triple-stranded sequences with varying GC content	3
2. Analysis of the Quenching Efficiency of Fluorophores	5
3. Fluorescence Characterization of the Triplex Switch.....	6
4. pH-Insensitive DNA Substrate Fluorescence Analysis	7
5. The 'OR' Logical Operation Strategy	8
6. The 'AND' Logical Operation Strategy	9
7. Fluorescent Analysis of Switchable Single Logic Computation Strategy.....	10
8. Efficiency Analysis of the 'AND' Logic Computation Strategy.....	11
9. Investigating the stability of DNA logic circuits.....	13
10. 'OR-OR' Logic Operation Strategy.....	14
11. 'AND-AND' Logic Operation Strategy.....	15
12. Switchable Cascaded Logic Operation Strategy Fluorescence Analysis.....	16
13. Brute-Force Cracking of the Dual-Layer DNA Molecular Firewall Access Control System.....	17
14. A dual-layer DNA firewall access control system with different pH response switches.....	18
15. Three-layer DNA Molecular Firewall Security Access Control System	19
16. Supplementary Tables.....	21

Materials and Methods

Assembly of the Reaction Substrates

Under acidic conditions, all DNA structures were dissolved and dispersed in 20 μL $1\times$ TAE/ Mg^{2+} buffer (pH 5.0) at a 1:1 molar ratio. Under alkaline conditions, the structures were prepared identically in 20 μL $1\times$ TAE/ Mg^{2+} buffer (pH 9.0), also at a 1:1 molar ratio. The structures were annealed using a PCR (polymerase chain reaction) thermal cycler with the following program: 95°C for 5 minutes, 65°C for 30 minutes, 50°C for 30 minutes, 37°C for 30 minutes, and 25°C for 30 minutes. For pH adjustment, glacial acetic acid was used to adjust the buffer to pH 5.0, and NaOH was used to adjust the buffer to pH 9.0.

Assembly of Single Logic Gate Reaction Substrates

To construct switchable logic function conversion substrates, F-ON/F-OFF were first pre-hybridized via the same thermal annealing method in buffers with the corresponding pH values. The pre-hybridized substrates were then mixed with other single-stranded DNA and double-stranded DNA at an equimolar concentration of 3 μM in $1\times$ TAE/ Mg^{2+} buffer, followed by incubation at 25 °C for 2 hours.

Assembly of Cascaded Logic Gate Conversion Reaction Substrates

To construct switchable cascaded logic function conversion substrates, F₁-ON (F₁-OFF/F₂-ON/F₂-OFF) were first pre-hybridized via the same thermal annealing method in buffers with the corresponding pH values. The pre-hybridized substrates were mixed with other double-stranded DNA, input strand IN₅, and input strands IN₃ and IN₄ (2.5 μM each) in $1\times$ TAE/ Mg^{2+} buffer. All components except IN₃ and IN₄ were present at an equimolar concentration of 2 μM . The mixture was subsequently incubated at 25 °C for 3 hours.

Cyclic Fluorescence Measurements

To monitor the conformational changes of the triplex switch, the true information module Tr and the switch module S were labeled with Cy5 and BHQ2 at their respective ends. All reactants (200 nM) were added to 100 μL of $1\times$ TAE/ Mg^{2+} buffer (pH 9.0), and the Cy5 fluorescence signal was monitored using a microplate reader (Spark 20M, Tecan, Switzerland). Following 5 minutes of monitoring, the buffer pH was adjusted to 5.0 with glacial acetic acid, with signal monitoring continued for another 5 minutes. The pH was then readjusted to 9.0 using sodium hydroxide, and monitoring was extended for an additional 5 minutes. This completed the reversible cycling of the DNA firewall molecular equipment.

Fluorescence Measurement of the Dual-layer DNA Molecular Firewall Access

Control System

First, 200 nM outer system substrate was mixed with the inner fluorescent substrate in $1\times$ TAE/ Mg^{2+} buffer, and the output fluorescence signal was monitored for 60 minutes using a microplate reader. Subsequently, after adjusting the pH, 200 nM inner system substrate (corresponding to the adjusted pH) was added, and the output

fluorescence signal was monitored for an additional 120 minutes via the same method.

Analysis of leakage values for switching efficiency in individual logical operations

For each condition, the leakage value (L) of the logical operation is calculated using the following formula (1).

$$L = \frac{F(l)}{F(max)} \quad (1)$$

Herein, L denotes the leakage value of the logical operation, $F(max)$ represents the maximum fluorescence value therein, and $F(l)$ is the maximum fluorescence value when the logical operation result is 0.

Supplementary Figures

1. Design and structural optimization of triple-stranded sequences with varying GC content

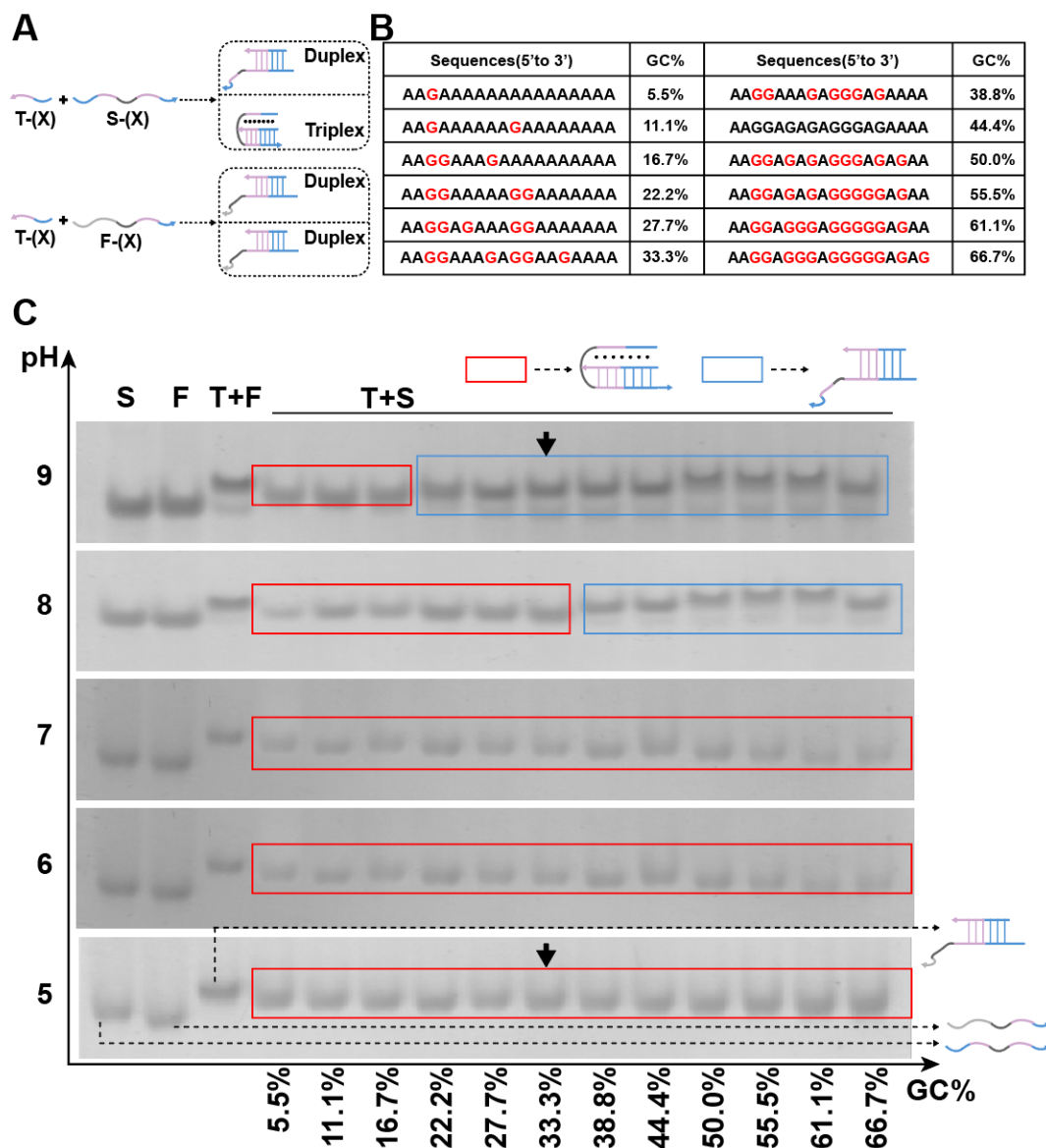


Fig.S1 Design and structural optimization of triple-helix sequences with varying GC content. (A) Schematic illustration of the triple-helix formation mechanism. X denotes the GC content in T-(X). (B) Twelve sets of triple-helix sequences and their corresponding GC content percentage. (C) Gel image showing triple-helix behavior under different pH conditions. The x-axis indicates the 12 triple-helix sets with different GC content, while the y-axis corresponds to pH values. Within a single gel: lanes 1-2 contain single strands, lane 3 displays the double helix formed by T-(X) and F-(X), and lanes 4-15 contain mixtures of all T-(X) and S-(X). Lanes with formed triple helices are marked with red boxes, and lanes without triple helices are marked with blue boxes. [S-(X)/F-(X)/T-(X)] = 6 μ M.

To visually monitor the formation of triple-helix structures under different pH conditions, three DNA strands with varying GC content were designed. In the absence of triple-helix formation, S-(X) remains open, corresponding to the double helix formed by T-(X) and F-(X). After triple-helix formation, the three single strands combine to form a higher molecular weight structure, resulting in a significantly reduced migration speed. This observation indicates that the amount of H⁺ required for triple-helix formation gradually decreases as the GC percentage decreases.

2. Analysis of the Quenching Efficiency of Fluorophores

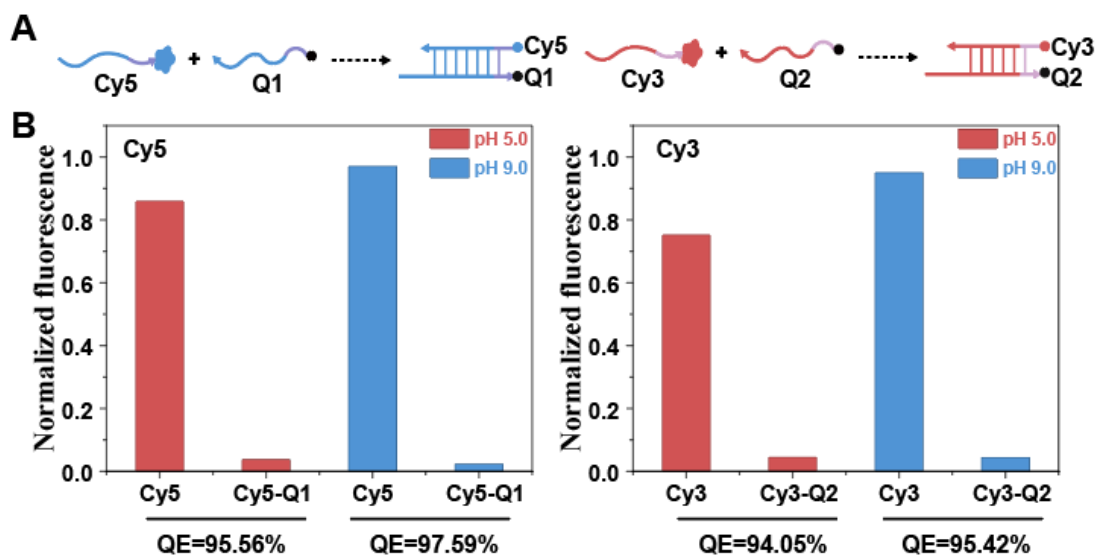


Fig.S2 Validation of fluorophore quenching efficiency. (A) Schematic diagram and (B) real-time fluorescence monitoring results for the quenching efficiency of pH-insensitive fluorescent reporters under different pH conditions. [Cy5, Cy3, and Q1, Q2] = 200 nM.

To minimize the influence of pH on fluorescence intensity, we validated the quenching efficiencies of Cy5 and Cy3 under different pH conditions. The experiment was performed at pH 5.0 and 9.0, where the fluorescence intensities of reporter molecules Cy5, Cy3, and their quenched counterparts (Cy5-Q1 and Cy3-Q2, with quenching strands Q1 and Q2 added) were measured. Quenching efficiencies for Cy5 were 95.56% at pH 5.0 and 97.59% at pH 9.0. For Cy3, the values were 94.05% at pH 5.0 and 95.42% at pH 9.0.

3. Fluorescence Characterization of the Triplex Switch

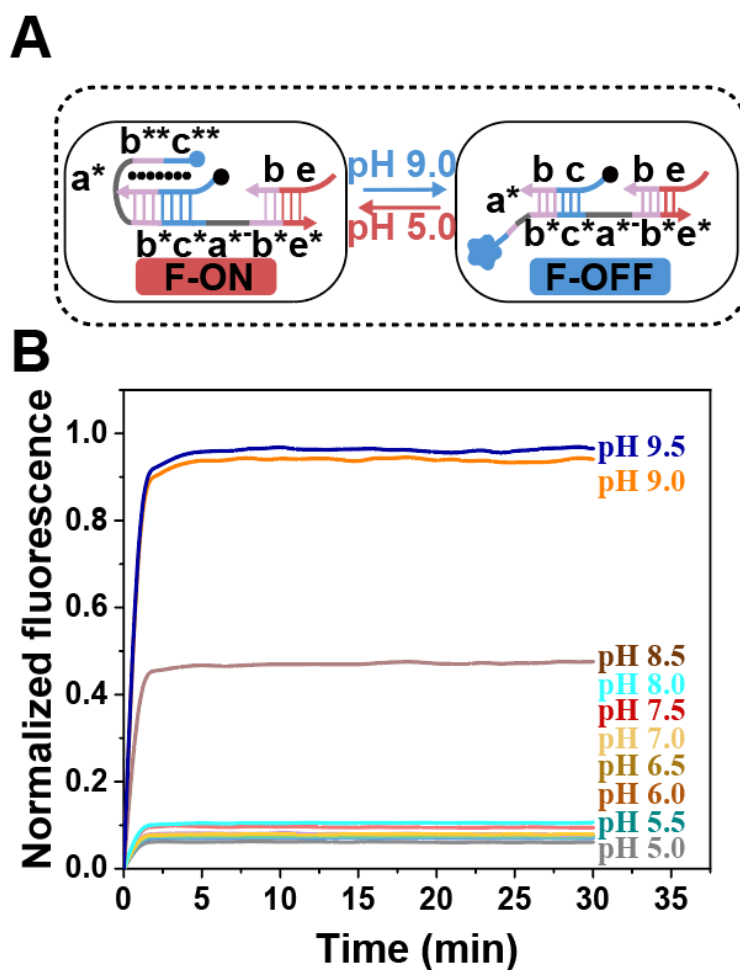


Fig.S3 DNA Triplex Switch. (A) pH response mechanism of the triplex switch and (B) real-time fluorescence monitoring results of the triplex switch. F-ON or F-OFF was prepared as a 200 nM solution in 100 μ L of $1\times$ TAE/Mg²⁺ buffer, with pH adjusted via sodium hydroxide or glacial acetic acid. Continuous fluorescence monitoring of the system was conducted for 30 minutes using a microplate reader. [F-ON/F-OFF] = 200 nM.

To verify the pH-responsive characteristics of the triplex switch, we labeled the switch module S with a Cy5 fluorophore and the true information module Tr with a BHQ2 quencher, enabling fluorescence quenching upon triplex formation. At pH 5.0, the G-C duplex and pyrimidine-rich domain involved in the triplex can assemble independently, forming the C-G-C⁺ triplex, with the triplex switch in the F-ON state. At pH 9.0, the triplex dissociates into a duplex, resulting in the triplex switch switching to the F-OFF state. Consequently, the fluorescence output of the triplex switch remains low under acidic conditions and gradually increases as pH rises.

4. pH-Insensitive DNA Substrate Fluorescence Analysis

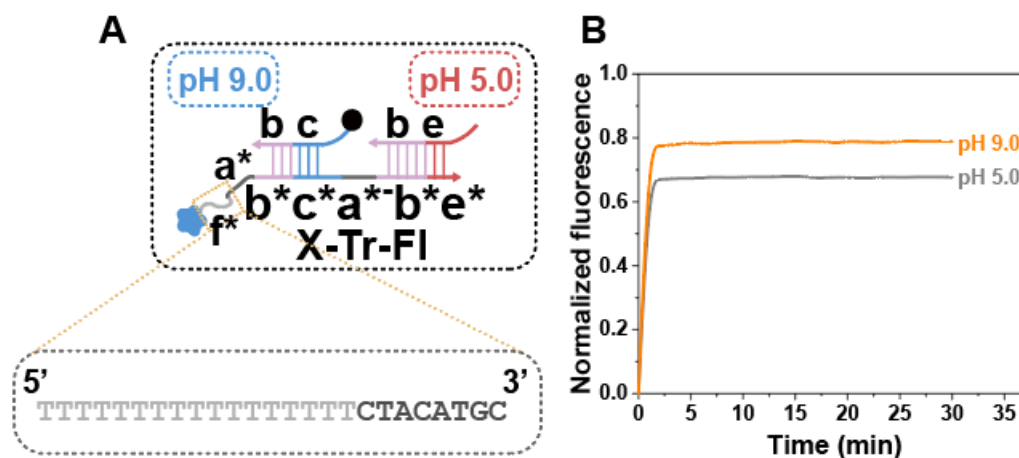


Fig.S4 pH-Insensitive DNA Substrate. (A) Schematic diagram and (B) real-time fluorescence monitoring results of the pH-insensitive switch under different pH conditions. This switch features a random sequence replacing the triplex-forming domain. [X-Tr-FI] = 200 nM.

A pH-insensitive switch was designed as a negative control for the pH-responsive triplex switch. Under acidic conditions, the random-sequence regions of the Tr and X domains (f*) cannot interact with (b-b*) and (c-c*), and thus triplex formation is prevented. The results showed that the substrates maintained high fluorescence output under both pH conditions, in the absence of C-G-C⁺ triplex formation. However, beyond the two types of Hoogsteen hydrogen bonds employed in the experiment (C-G-C⁺ and T-A-T), several other types exist that can form unintended triplexes, and these account for the slight reduction in fluorescence intensity observed for the pH-insensitive DNA substrates at pH 5.0.

5. The 'OR' Logical Operation Strategy

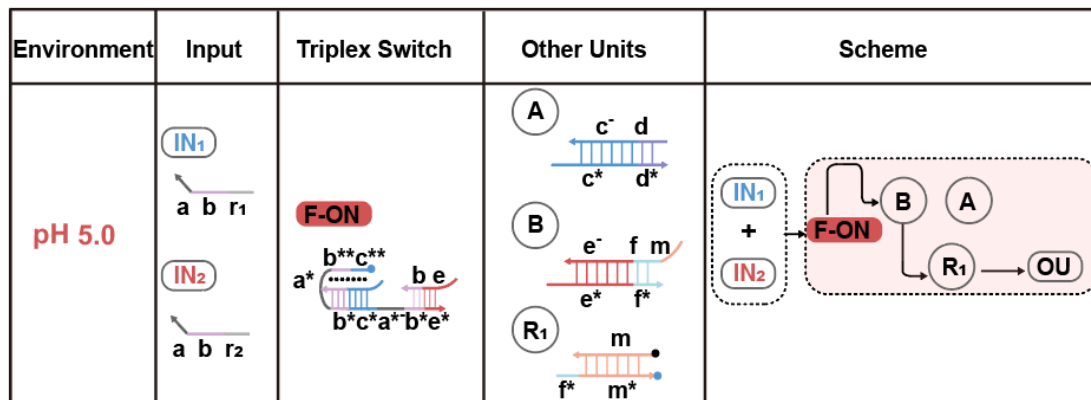


Fig.S5 The working mechanism of the 'OR' logical operation strategy at pH 5.0. First column: pH environment. Second column: Inputs. Third column: Triplex switch. Fourth column: Reaction units A, B, and fluorescent reporter R₁. Fifth column: Switchable DNA logic operation schemes at pH 5.0.

An output of '1' is generated only when IN₁ or IN₂ is present, indicating the execution of an 'OR' logic operation. Specifically, IN₁ or IN₂ first recognizes the triplex domain (a*-b*), which triggers the dissociation of strand (be). The dissociated strand (be) then binds to reaction unit B, subsequently inducing the dissociation of strand (e⁻fm). Finally, the free strand interacts with the fluorescent reporter R₁ and displaces the quencher strand (m), thereby generating the fluorescent output signal.

6. The 'AND' Logical Operation Strategy

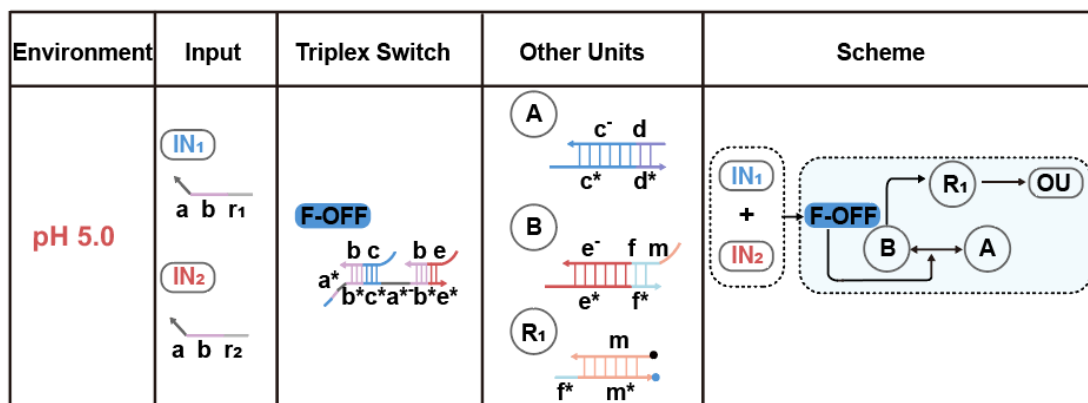


Fig.S6 The working mechanism of the 'AND' logic operation strategy at pH 9.0. First column: pH environment. Second column: Inputs. Third column: Triplex switch. Fourth column: Reaction units A, B, and fluorescent reporter R₁. Fifth column: Switchable DNA logic operation schemes at pH 9.0.

An output of '1' is generated only when both IN₁ and IN₂ are present, indicating the execution of an 'AND' logic operation. Specifically, IN₁ and IN₂ first recognize their respective triplex domains (a*b*) and (a*b*), triggering the dissociation of strands (be) and (bc). Subsequently, strand (be) binds to reaction unit B, which in turn induces the dissociation of strand (e⁻fm). Finally, the free strand (e⁻fm) interacts with the fluorescent reporter R₁ and displaces the quencher strand (m), thereby generating a fluorescent output signal.

7. Fluorescent Analysis of Switchable Single Logic Computation

Strategy

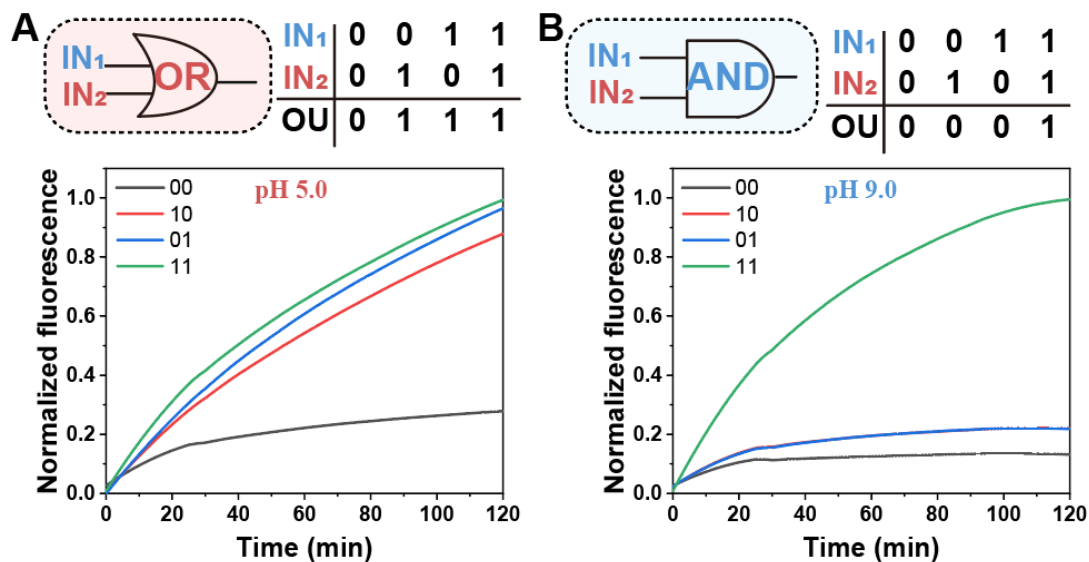


Fig.S7 Real-time fluorescence of the switchable single logic computation strategy under (A) pH 5.0 and (B) pH 9.0 conditions.

Under pH 5.0 conditions, an output of '1' is generated only when either IN₁ or IN₂ is present, indicating the execution of an 'OR' logic operation. Under pH 9.0 conditions, an output of '1' is generated only when both IN₁ and IN₂ are present, indicating the execution of an 'AND' logic operation.

8. Efficiency Analysis of the 'AND' Logic Computation Strategy

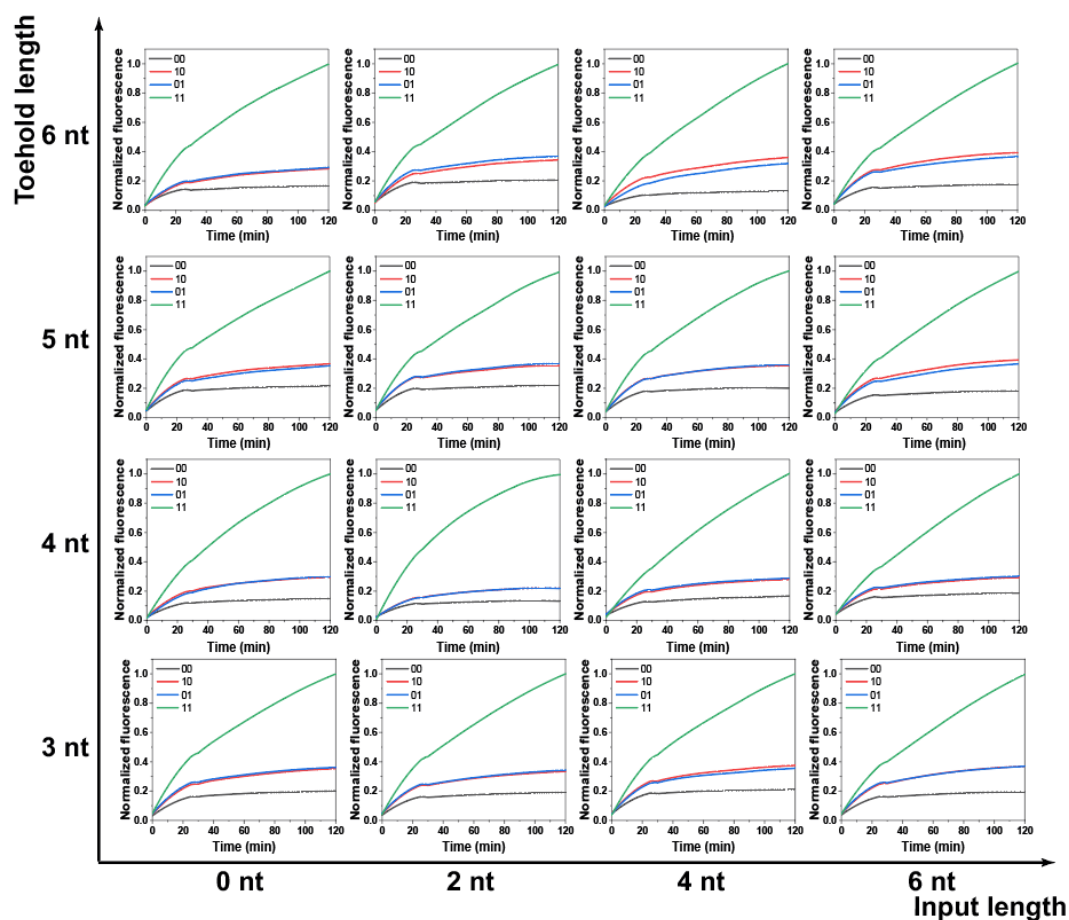


Fig.S8 Molecular equipment short toehold domain (a^{*}-) length (from 3 nt to 6 nt), domain (b) tail length (from 0 nt to 6 nt) normalized fluorescence.

To improve the accuracy and robustness of the 'AND' logic operation, we reduced circuit leakage by modifying the length of the toehold domain (a^{*}-) of triplex switch F-OFF and F-ON, and the tail length of the input strand-binding domain (b). Optimal conditions were identified based on Equation (1) and Table 1. The results indicate that the logic operation achieves optimal performance when the toehold domain length is 4 nt and the tail length of the input strand-binding domain is 2 nt.

Table S1. Leakage values of 'AND' logic operations for different schemes.

Input \ Toehold	0 nt	2 nt	4 nt	6 nt
3 nt	0.35323	0.33443	0.35526	0.36880
4 nt	0.29667	0.21817	0.27889	0.29329
5 nt	0.35400	0.35432	0.35438	0.36662
6 nt	0.28375	0.34316	0.31900	0.36633

Calculations using Equation 1 show that the leakage value is the lowest (0.21817) at a toehold length of 4 nt and an input length of 2 nt, indicating that the 'AND' logic operation exhibits the highest efficiency under these conditions.

9. Investigating the stability of DNA logic circuits.

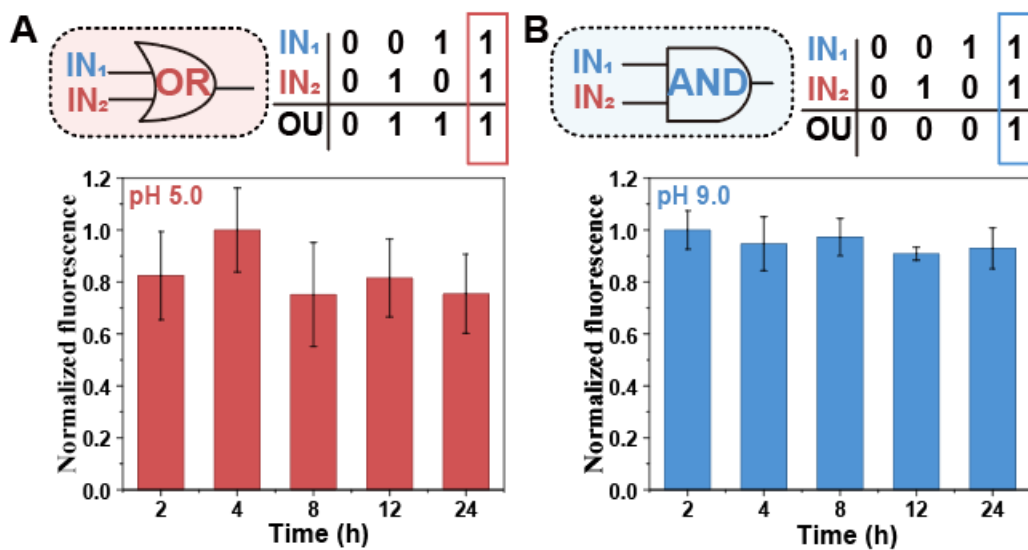


Fig.S9 Final fluorescence intensity plots of the switchable individual logic circuit after reacting for 2, 4, 8, 12, and 24 hours under conditions of (A) pH 5.0 and (B) pH 9.0.

Upon simultaneous addition of IN₁ and IN₂, the final fluorescence intensity was monitored over time. The persistent high signal observed at 24 hours substantiates the robust stability of the designed DNA logic circuit.

10. 'OR-OR' Logic Operation Strategy

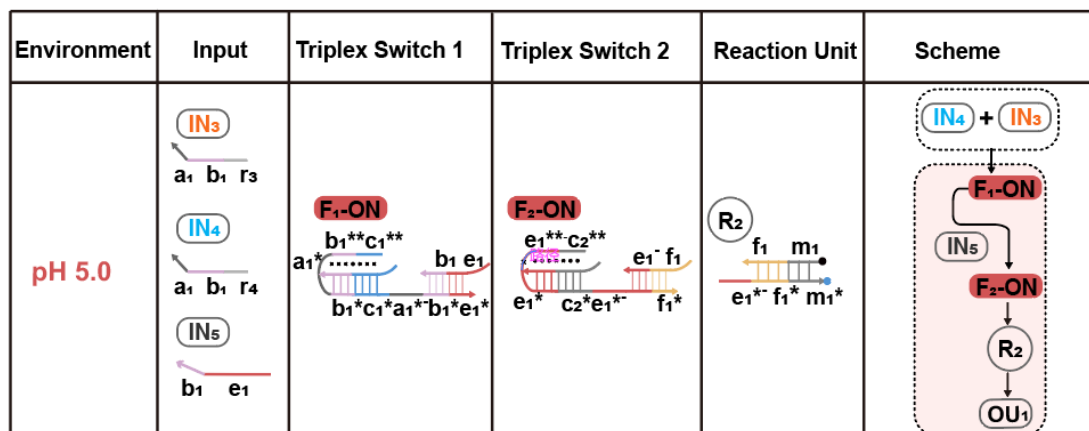


Fig.S10 The working mechanism of the 'OR-OR' logic operation strategy at pH 5.0. First column: pH environment. Second column: Inputs. Third column: First set of triplex switches. Fourth column: Second set of triplex switches. Fifth column: Fluorescence reporter R_2 . Sixth column: Scheme for switchable DNA cascade logic operations at pH 5.0.

An output of '1' is generated only when any of IN_3 , IN_4 , or IN_5 is present, indicating the execution of a cascaded 'OR-OR' logic operation. Specifically, IN_3 or IN_4 first recognizes the F_1 -F domain ($a_1^*b_1^*$) of the triplex switch, triggering the dissociation of strand (b_1e_1). Subsequently, the free strand (b_1e_1) or IN_5 mediates a strand displacement reaction with F_2 -F, inducing the dissociation of strand (e_1f_1). Finally, the free strand (e_1f_1) interacts with the fluorescent reporter R_2 and displaces the quencher strand (f_1m_1), thereby generating a fluorescent output signal.

11. 'AND-AND' Logic Operation Strategy

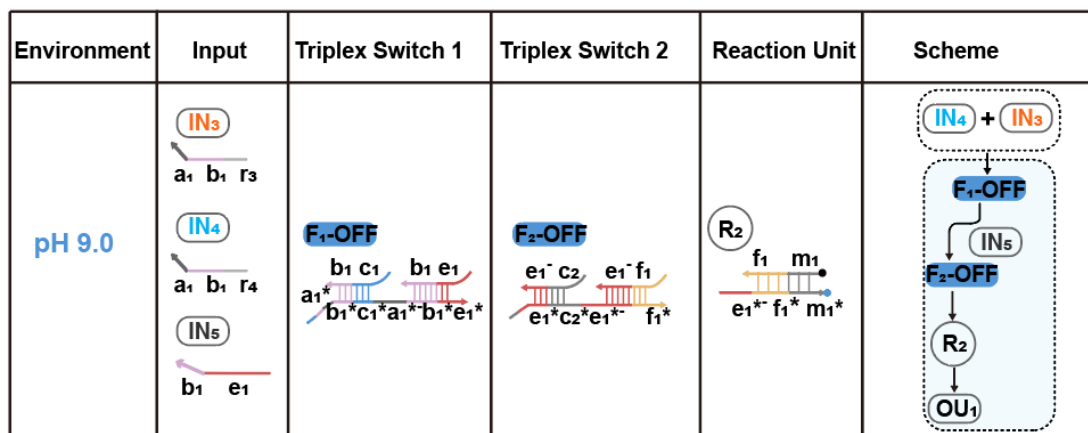


Fig.S11 The working mechanism of the 'AND-AND' logic operation strategy at pH 9.0. First column: pH environment. Second column: Inputs. Third column: First set of triplex switches. Fourth column: Second set of triplex switches. Fifth column: Fluorescence reporter R2. Sixth column: Scheme for switchable DNA cascade logic operations at pH 9.0.

An output of '1' is generated only when all of IN₃, IN₄, and IN₅ are present, indicating the execution of a cascaded 'AND-AND' logic operation. Specifically, IN₃ and IN₄ first collectively recognize their respective F₁-T domains (a₁*·b₁*) and (a₁*b₁*) of the triplex switch, triggering the dissociation of strands (b₁e₁) and (b₁c₁). Subsequently, the free strand (b₁e₁), together with IN₅, mediates a strand displacement reaction with the downstream F₂-T, thereby displacing strands (e₁f₁) and (e₁c₂). Finally, the free strand (e₁f₁) interacts with the fluorescent reporter R₂ and displaces the quencher strand (f₁m₁), thereby generating a fluorescent output signal.

12. Switchable Cascaded Logic Operation Strategy Fluorescence

Analysis

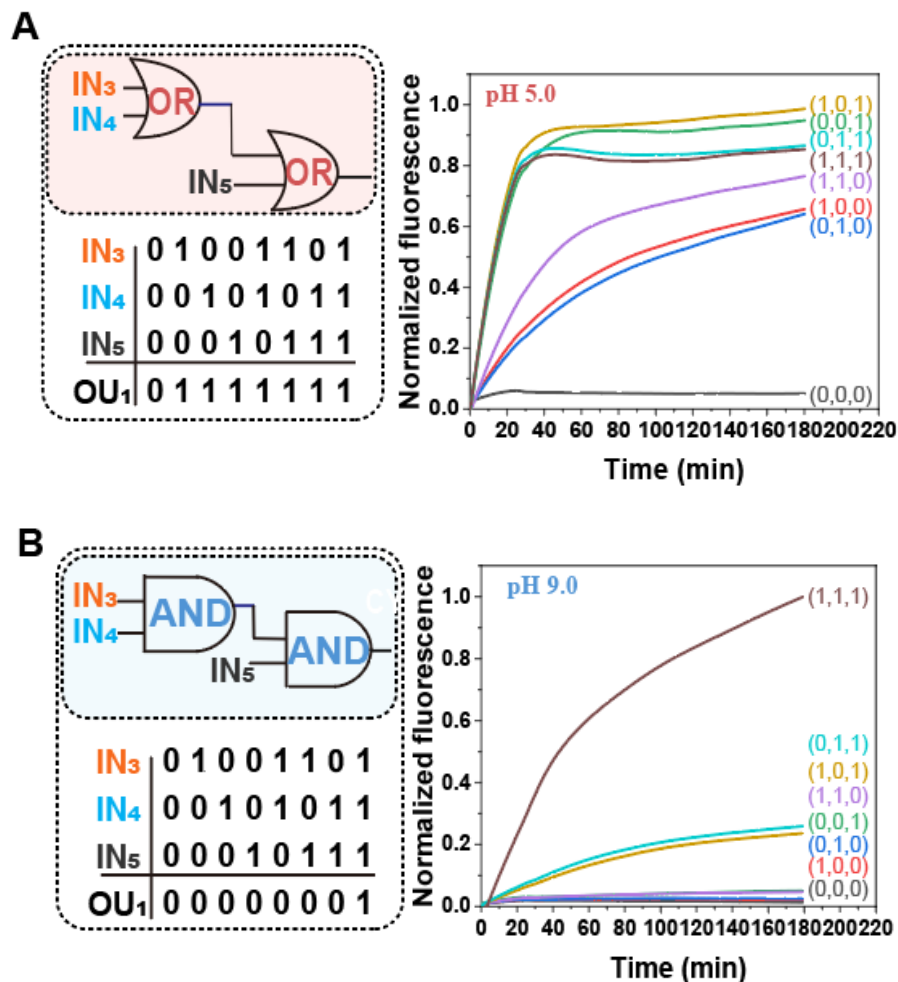


Fig.S12 Real-time fluorescence detection of the switchable cascaded logic operation strategy: (A) under pH 5.0 and (B) under pH 9.0.

Under pH 5.0 conditions, an output of '1' is generated only when any of IN₃, IN₄, or IN₅ is present, indicating the execution of a cascaded 'OR-OR' logic operation. Under pH 9.0 conditions, an output of '1' is generated only when all of IN₃, IN₄, and IN₅ are present, indicating the execution of a cascaded 'AND-AND' logic operation.

13. Brute-Force Cracking of the Dual-Layer DNA Molecular Firewall Access Control System

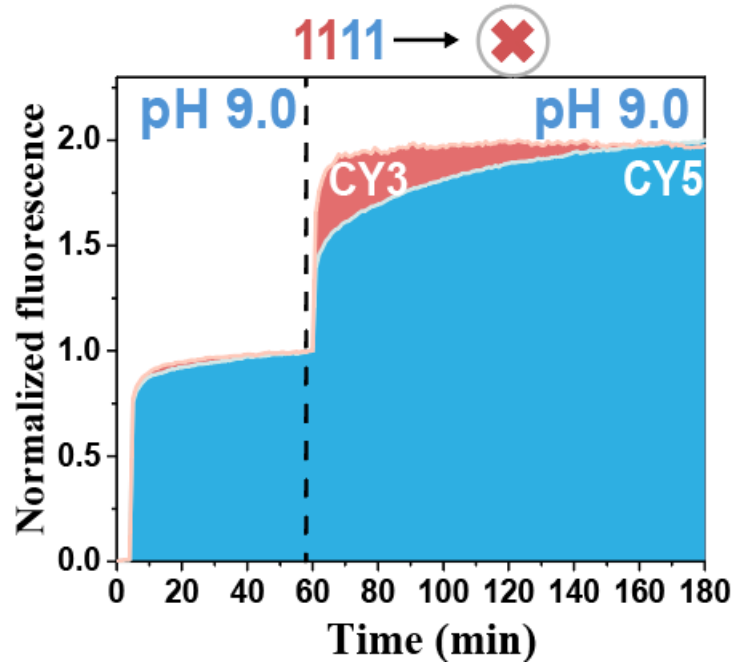


Fig.S13 Brute-force cracking real-time fluorescence detection of the dual-layer DNA molecular firewall access control system.

When an attacker inputs an excessive amount of key K_1 under alkaline conditions, although the true address information (Tr_1 and Tr_2) dissociates, the false address information ($F1_1$ and $F1_2$) also dissociates simultaneously. Therefore, while the attacker obtains the true information, they also gain access to false information, and the final result derived from combining the two remains incorrect.

14. A dual-layer DNA firewall access control system with different pH response switches

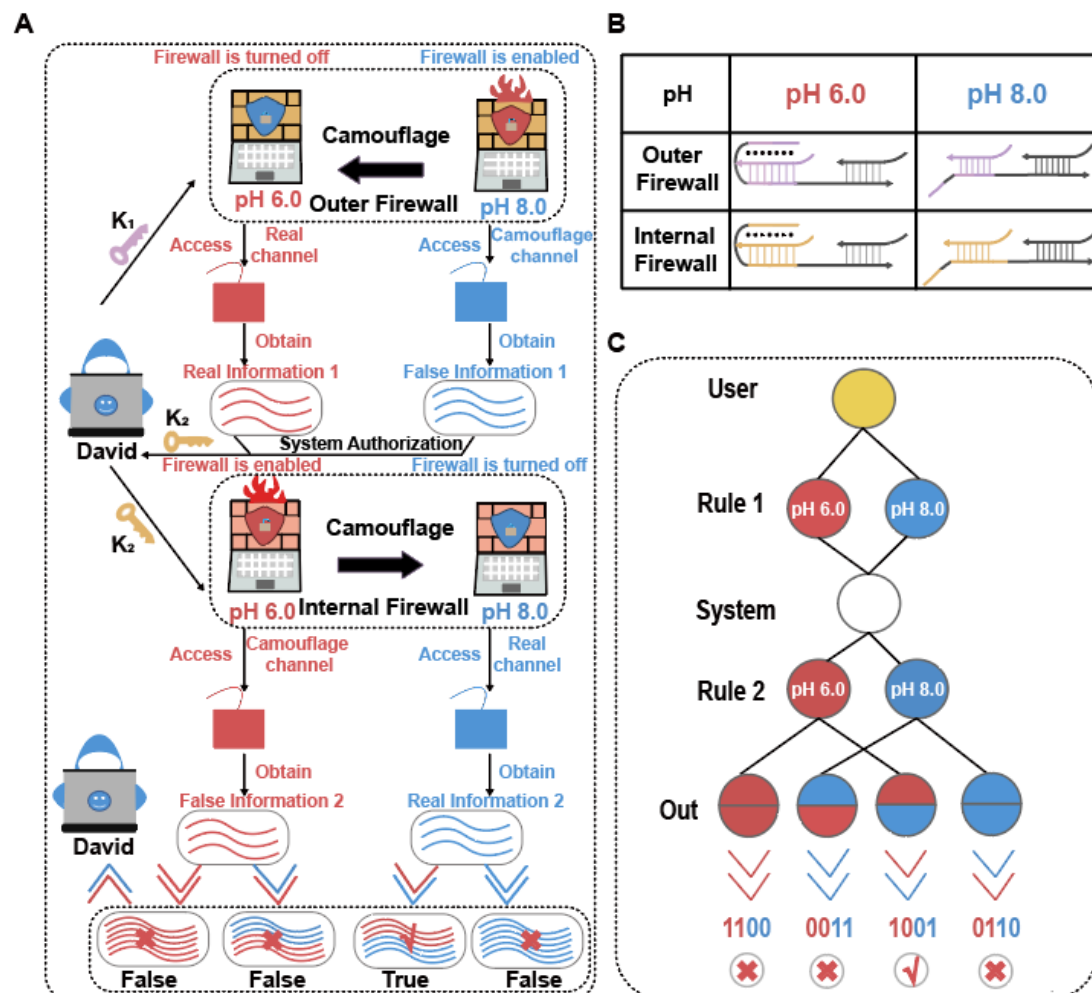


Fig.S14 Two-layer DNA molecule security access control system with different pH switches. (A) System concept diagram; (B) Schematic diagram of the molecular firewall status under different pH environments; (C) Flowchart of user access to the system and schematic diagram of obtaining different result information;

By rationally designing the triplet sequence—for example, adjusting the proportion of protonated cytosine in the C-G-C⁺ structure—it is possible to construct switching units with different and precise pH response thresholds over a wide pH range, thus surpassing the currently limited two-state configuration.

15. Three-layer DNA Molecular Firewall Security Access Control System

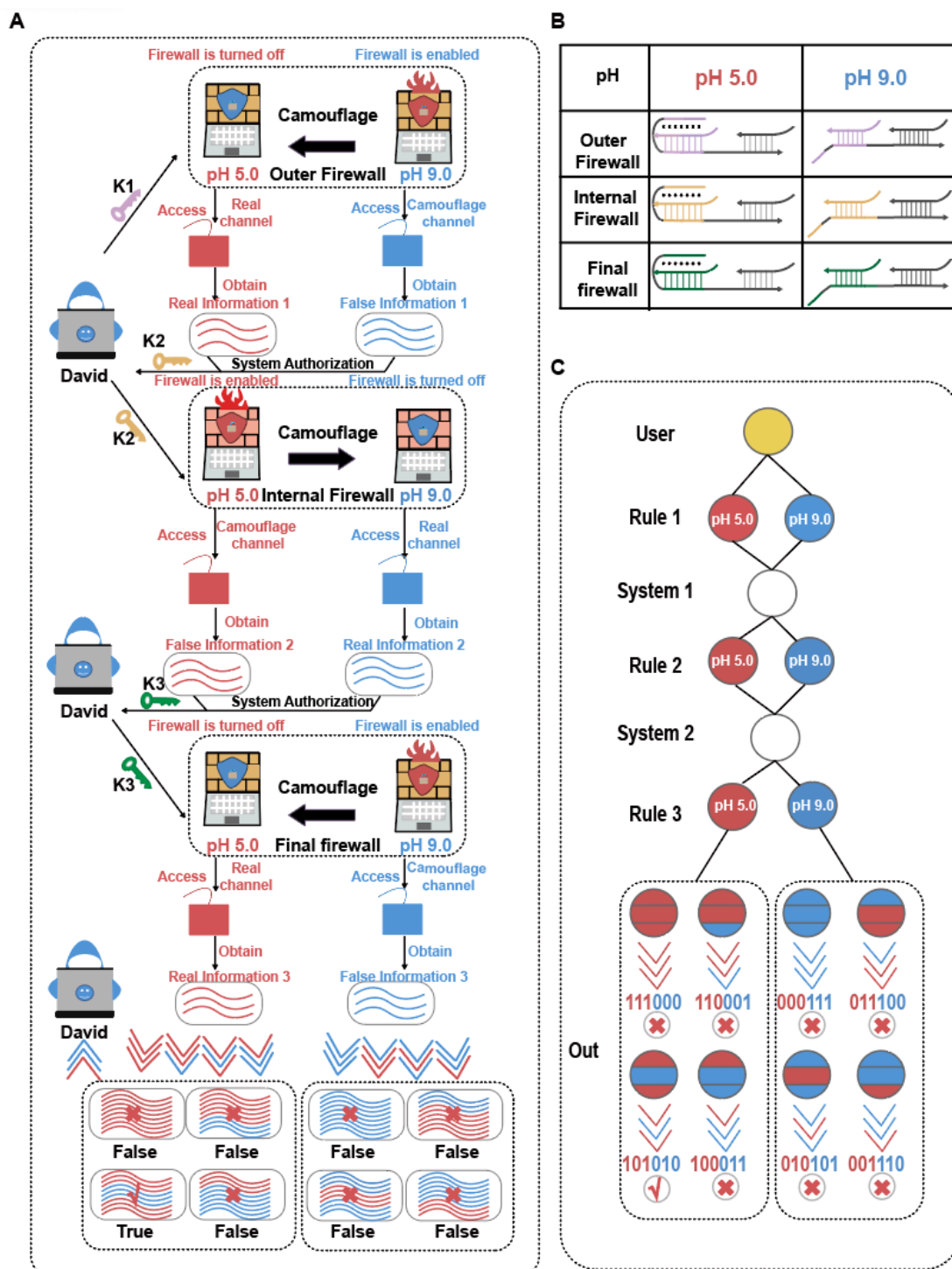


Fig.S15 Three-layer DNA molecular firewall security access control system. (A) System concept diagram; (B) Schematic diagram of the state of the three-layer molecular firewall under different pH conditions; (C) User access system flowchart and schematic diagram of obtaining different result information;

The three-layer firewall operates sequentially at different layers, with the output of each layer triggering the next, forming a multi-factor authentication path. The number of possible state combinations increases by 2^n , where n is the layer number. For example, a layer 3 system will provide 8 (2^3) state combinations, a layer 4 system will provide 16 (2^4) combinations, and so on. This exponential expansion indicates that our two-layer firewall is not limited to 2×2 states.

16. Supplementary Tables

Table S2. Nucleotide sequences for triplex switch construction.

Stand	Sequence (from 5' to 3')
S	Cy5- TTCCCTTCTCCTTCTTTTGTACATGCTTTTCTTCCTCTTCCTTC TATAACAACATGCTTTTCTTCCTCTCAC
Tr	BHQ2-GAGATGGTAAGGAAAGAGGAAGAAAA
Fl	AATGATTGTGTGAGAGGAAGAAAA
X	TTTTTTTTTTTTTTTTTTGTACATGCTTTTCTTCCTCTTCCTTC ATAACAACATGCTTTTCTTCCTCTCAC

Table S3. Nucleotide sequences for validating the camouflage mechanism of the triplex switch.

Stand	Sequence(from 5' to 3')
S	TTCCTTTCTCCTTCTTTTGTACATGCTTTTCTTCCTCT TTCCTTCTATAACAACATGCTTTTCTTCCTCTCAC
Tr	GAGATGGTAAGGAAAGAGGAAGAAAA
Fl	AATGATTGTGTGAGAGGAAGAAAA
K	AGAGGAAGAAAAGCATGTACAAAAG
B	BHQ2-AGGAGAGATGGTAAG
B*	CCTCTTTCCTTACCATCTCTCCT-Cy5

Table S4. Nucleotide sequences for switchable single-logic operation strategies.

Stand	Sequence(from 5' to 3')
S	6 nt TTCCTTTCTCCTTCTTTTTGTACATGCTTTTCTTCCTCTTT CCTTCTATAACAACATGCTTTTCTTCCTCTCAC
	5 nt TTCCTTTCTCCTTCTTTTTGTACATGCTTTTCTTCCTCTTT CCTTCTATAACACATGCTTTTCTTCCTCTCAC
	4 nt TTCCTTTCTCCTTCTTTTTGTACATGCTTTTCTTCCTCTTT CCTTCTATAACAATGCTTTTCTTCCTCTCAC
	3 nt TTCCTTTCTCCTTCTTTTTGTACATGCTTTTCTTCCTCTTT CCTTCTATAACATGCTTTTCTTCCTCTCAC
Tr	GAGATGGTAAGGAAAGAGGAAGAAAA
Fl	AATGATTGTGTGAGAGGAAGAAAA
IN ₁	6 nt CTTATAGAAGGAAAGAGGAAGAAAAGCATGTACAAAAG
	4 nt CATAGAAGGAAAGAGGAAGAAAAGCATGTACAAAAG
	2 nt CAGAAGGAAAGAGGAAGAAAAGCATGTACAAAAG
	0 nt CAAGGAAAGAGGAAGAAAAGCATGTACAAAAG
IN ₂	6 nt ATTATAGAAGGAAAGAGGAAGAAAAGCATGTACAAAAG
	4 nt AATAGAAGGAAAGAGGAAGAAAAGCATGTACAAAAG
	2 nt AAGAAGGAAAGAGGAAGAAAAGCATGTACAAAAG
	0 nt ACAAGGAAAGAGGAAGAAAAGCATGTACAAAAG

A	c-d	AGGAGAGATGGTAAG
	c*d	CCTCTTTCCTTACCATCTCTCCT
B	e-fm	GTAAGTTTGGTGTGGATAATGATTGTG
	e*f*	CCTCTCACACAATCATTATCCA
	m	BHQ2-GAGTAAGTTTGGTGTG
	f*m*	TATCCAACACCAAACCTTACTC-Cy5

Table S5. Nucleotide sequences for switchable cascade logic operation strategies.

Stand	Sequence(from 5' to 3')
F ₁ -ON/F ₁ - OFF	$c_1^{**}b_1^{**}a_1^{*}b_1^{*}$ $c_1^{*}a_1^{*}b_1^{*}e_1^{*}$ TTTCCTTCTTTTCTCCTTTCATCATATTCCTCTTTTC TTCCTTTCAATTACTCATATTCCTCTTTTCTCTTCCT TTCAATT
	b_1c_1 GTATACATAAAGGAAGAAAAGAGGAA
	b_1e_1 ATGAATAGGAAAGAGAAGAGAAAAGAGGAA
F ₂ -ON/F ₂ - OFF	$c_2^{**}e_1^{**}e_1^{*}$ $c_2^{*}e_1^{*}f_1^{*}$ TCCTTTCTCTTCTCTTTTTTCTCTTTTCTCTTCTCT TTCCTATTCATAACCTCTTTTCTCTTCTCCCTATT
	e_1c_2 ATGTATGAAGGAAAAGAGAAGAGAAAA
	e_1f_1 AATGATAATAGGGAGAAGAGAAAA
f_1m_1	BHQ2-CCAATGATAATAGGGAG
$e_1^{*}f_1^{*}m_1^{*}$	CTCTTCTCCCTATTATCATTGG-Cy5

Table S6. Nucleotide sequences for construction of the dual-layer DNA molecular firewall access control system.

Stand	Sequence(from 5' to 3')
FI ₁	TGCTATTCCAAGGAAAGAAGGAGAAAA
Tr ₁	AATGCTATTACTTACAGAAGGAGAAAA
Tr ₂	TATACATAAAGGAAAAGAAGAGGAA
FI ₂	CTAATGAATAGGTAAAGAAGAGGAA
a ₂ b ₃	AAACAAAGGAAAGAAGGAGAAAAGCATGTACAAAAG
OU ₂	Cy3-GAAGAGGAATGCTATTACTTAC
e ₂ *a ₃ *	TCCTTCTGTAAGTAATAGCATTCC-BHQ2
OU ₃	Cy5-GAAGAGGAATGCTATTCCAAGG
c ₃ *a ₃ *	CTTCTTTCCTTGGAATAGCATT-BHQ2
a ₃ y ₄	AAAAGGAAAAGAAGAGGAATGCTATG
e ₂ *-a ₃ *y*	GTAAGTAATAGCATTCCCTCTTCTT
c ₃ *-a ₃ *y*	CCTTGGAATAGCATTCCCTCTTCTT
OU ₄	Cy3-GGCTAATGAATAGGT

$e_3^*m_3^*$	TCTTCTTTACCTATTCATTAGCC-BHQ2
OU ₅	Cy5-GGTATACATAAAGGA
$c_4^*f_2^*$	CTCTTCTTTTCCTTTATGTATACC-BHQ2
$c_3^*b_3^*a_2^*b_3^*$	TTCCCTTCTTCCTCTTTTGTACATGCTTTTCTCCTTCTTTCC
$c_3^*a_2^*b_3^*e_2^*$	TTTGTTTGAGATGCTTTTCTCCTTCTGTACACGGT
$c_4^*b_4^*a_3^*b_4^*$	TTTCCTTTTCTTCTCCTTCATAGCATTCTCCTTCTTTTCCTTT
$c_4^*a_3^*b_4^*e_3^*$	TAAGGACAGCATTCTCCTTCTTTACCTTCAGG